DGS Resonators Form Compact Filters

Article *in* Microwaves and Rf · March 2015

2 authors:

Ahmed Boutejdar

Ahmed Abdel-monem Ibrahim
Minia University

Design Feature

DR. AHMED BOUTEJDAR | Associate Professor
Chair of Microwave and Communication Engineering, Otto Von Guericke University of Magdeburg, Magdeburg, Germany; e-mail: boutejdar69@gmail.com, www.uni-magdeburg.de

AHMED A. IBRAHIM | Lecturer
Communications and Electronic Engineering Department, Minia University, El-Minia, Eqypt, e-mail: ahmedabdel_monem@mu.edu.eg, www.minia.edu.eg

DR. EDMUND P. BURTE | Professor, Chair of Semiconductors and Sensors
Otto Von Guericke University of Magdeburg, Magdeburg, Germany; e-mail: edmundburte@ovgu.de, www.ovgu.de

DGS RESONATORS Form Compact Filters

The use of DGS resonators can help to shrink bandpass and bandstop filters—at the same time achieving both high selectivity and sharp transitions from passbands to stopbands.

Rapid growth of modern communication systems has encouraged the development of a number of different compact filters with special specifications, such as multiband operation.[1] Defected ground structures (DGS) have been employed in a growing number of RF/microwave components, including power dividers/combiners and filters, to achieve high performance with small size.[2-9]

A DGS is constructed by etching a defected pattern on a printed-circuit board's (PCB) metallic ground plane, changing the effective capacitance and inductance of a microstrip line formed on that circuit and altering the current distribution on the ground plane. By consequence, a DGS exhibits slow-wave characteristics and rejects harmonics in microwave circuits, improving the performance of filters and other microwave circuits.

An inductive-capacitive (LC) equivalent circuit can be used to model a DGS resonator for calculations and circuit simulations.[10-14] Different DGS resonators used in microwave filters include low-pass, bandpass, and bandstop circuits consisting of certain resonators or transmission lines, with the DGS added to improve filter performance. For example, a bandstop filter (BSF) can be implemented using all shunt stubs or by means of series-connected high-low stepped impedance lines.

DGS resonators have been proposed for improving the spurious responses of microstrip filters.[15-18] When attempting to achieve good performance with high selectivity, microwave

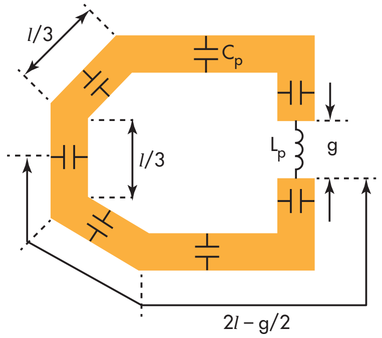

1. This represents a proposed DGS resonator and its equivalent-circuit model.

> "Different DGS resonators used in microwave filters include low-pass, bandpass, and bandstop circuits consisting of certain resonators or transmission lines, with the DGS added to improve filter performance."

filters with transmission zeros should be designed.[2] Having transmission zeros at finite frequencies provides sharp cutoff slopes at transitions from passbands to stopbands, which can be useful for many applications.

To demonstrate the present design approach, both compact microstrip bandstop and bandpass filters (BPFs) will be spotlighted—each based on the use of two DGS resonators. The filters are compact and also provide sharp transition responses. The design technique will be explored through the use of commercial circuit simulation software, including popular simulators from Applied Wave Research (www.awrcorp.com) and Computer Simulation Technology (CST; www.cst.com), with measurements of prototypes compared with the simulations to see how closely they match.

A DGS resonator etched in a metal ground plane is shown in *Fig. 1*. The open-loop DGS resonator features sharp angles to reduce passive parasitic capacitances and decrease the size of the DGS cell. The open-loop DGS resonator consists of two capacitive arms that are connected via a rectangular metal stub. The etched DGS achieves an equivalent capacitance while the metal area between the two arms achieves an equivalent inductance. The size of the open-loop DGS arm equals 4l – g from *Fig. 1*. The proposed DGS resonator corresponds to the equivalent-circuit LC model[3] demonstrated in *Fig. 1*.

Values for the resonator's inductor and capacitor, L_p and C_p, can be computed by means of Eqs. 1 and 2[7]:

$$C_p = 5f_c/\pi(f^2_0 f^2_c)\text{pF} \quad (1)$$

$$L_p = 250/C(\pi f_0)^2\text{nH} \quad (2)$$

where:
f_c = the cutoff frequency (in GHz), and
f_0 = the resonant frequency (in GHz) calculated from the transmission characteristics of the quasi-ring DGS slot.

When the quasi-ring DGS slot in the ground plane of *Fig. 1* is excited by a 50-Ω transmission line, it performs as a parallel LC resonant circuit[10] and also exhibits one-pole bandstop characteristics *(Fig. 2)*. To better understand how changes in the dimensions of the DGS cell affected the behavior of the bandstop filter, a parametric analysis was conducted.

For example, *Fig. 2* includes the effects of changes in stub width, g, in the open-loop-ring DGS slot on the resonant frequencies of the filter. By changing the width of g, the cutoff frequency and attenuation pole can be readily modified.

The length of the gap (arm) controls the effective capacitance of the microstrip line. As the metal stub width g increases, the cutoff frequency and the attenuation poles shift to higher frequencies. As *Fig. 2* shows, the resonant frequency jumps from 4.0 to 6.5 GHz as g increases from 3 to 7 mm. As g increases, the effective inductance decreases, so the resonant frequency increases. In this way, it can be seen that the stub width g controls the effective inductance, which in turn controls the resonant frequency.

Figure 3 contains a three-dimensional (3D) view of the proposed BSF. The filter consists of two overlapped DGS resonators etched into the bottom layer of the filter circuit, where distance,

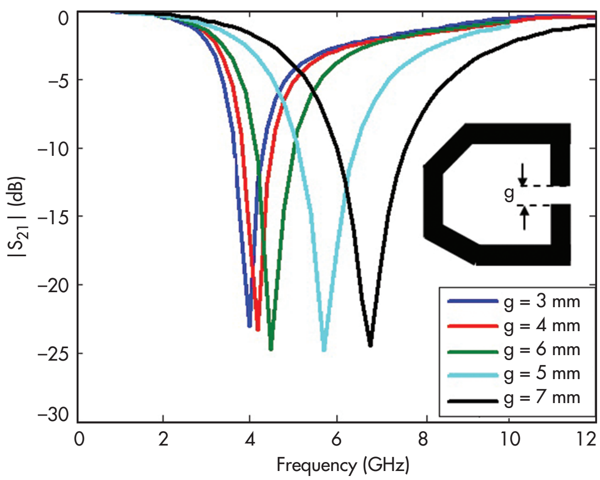

2. These simulations of S_{21} insertion loss show the impact of changing gap width g.

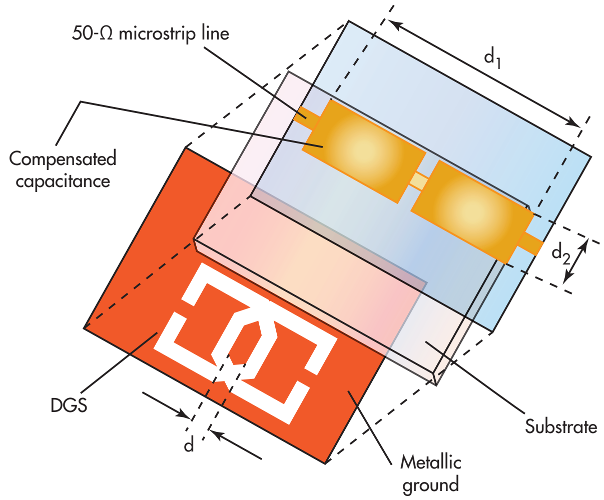

3. This is a three-dimensional (3D) view of the DGS bandstop filter (BSF).

d, equals 2.5 mm. In addition, two compensating microstrip capacitances on the top layer are connected by means of a 50-Ω microstrip line. Electrical coupling between the two DGS resonators is employed to improve filter performance.

The proposed bandstop filter was fabricated and measured with a model HP8722D vector network analyzer (VNA) from Agilent Technologies (now Keysight Technologies; www.keysight.com). The filter was printed on Rogers RO4003 PCB material from Rogers Corp. (www.rogerscorp.com) with a relative dielectric constant, ε_r, of 3.38 measured at 10 GHz through the z-axis (thickness) of the material.

The PCB material had a thickness, h, of 0.813 mm. *Figure 4* is a photograph of the fabricated BSF.

This use of DGS resonators for the BSF makes possible an extremely compact filter. A total area of $0.50\lambda_g \times 0.25\lambda_g$ is occupied by the filter circuitry, where the wavelength λ_g equals 38.5 mm. *Figure 5* offers a comparison of measured performance with simulations from the commercial simulation software. It is clear from the simulations that the filter's center frequency $f_0 = 4.1$ GHz with a cutoff frequency $f_c = 2.5$ GHz.

The simulated 3-dB stopband bandwidth equals 2.7 GHz. The simulation results showed that the designed filter has good transition characteristics and a symmetrical response *(Fig. 5)*. In addition, the measured stopband return loss and insertion loss are quite respectable: less than −20 dB and 0.7 dB, respectively.

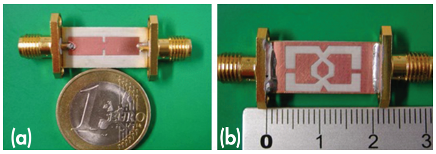

4. These photographs show the fabricated DGS BSF: (a) top and (b) bottom.

The results of *Fig. 5* show that the use of electric coupling between the two DGS resonators serves to enhance the performance of the BSF, arming it with a wide rejection band and sharp transition from the stopband to the passband. The design strategy produces reflection transmission zeros on both sides of the stopband center frequency to help increase the selectivity of the filter.

Less-than-positive results were achieved for the BPF; *Fig. 6* offers a 3D view. The structure has a small gap with separation distance, s, equal to 5 mm between the microstrip feeds to the admittance inverter, J. In this case, the transmission characteristics are inverted, causing the structure to act as a BPF. *Figure 7* offers results of a commercial electromagnetic (EM) simulation program used to analyze this structure. Simulated results reveal that the filter circuitry behaves much like a BPF, with center frequency f_0 at 5 GHz.

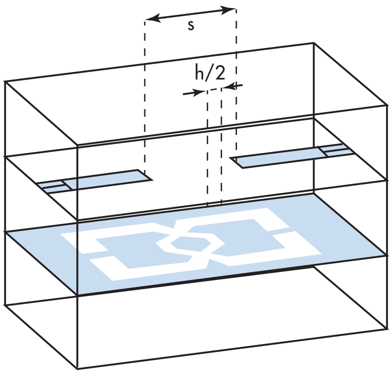

6. This is a 3D view of the DGS BPF formed from the use of a J-inverter with the BSF.

The return loss is predicted as being more than 20 dB across the passband from 4.5 to 5.7 GHz, while the simulated passband insertion loss is less than 1.9 dB from 4.5 to 5.5 GHz. Also, there's no spurious passband at $2f_0$. From the simulation results, two transmission zeros on both sides of the passband can be observed at 3.3 and 11.6 GHz. The BPF simulations show undue losses in the passband and a less-than-ideal upper-transition response. This poor performance can be attributed to poor coupling between the two adjacent DGS resonators.

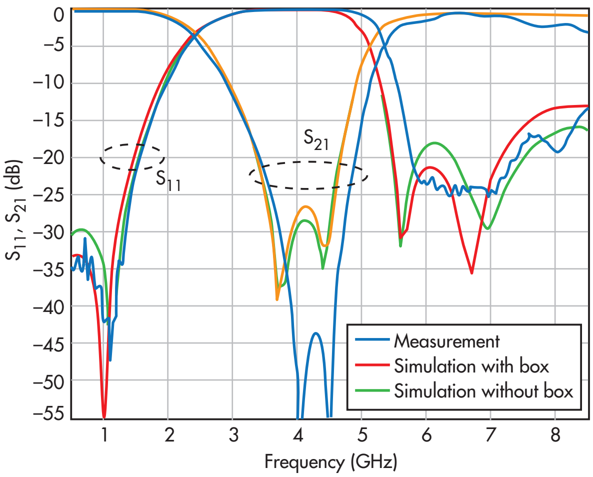

5. These traces are measured and simulated S-parameters.

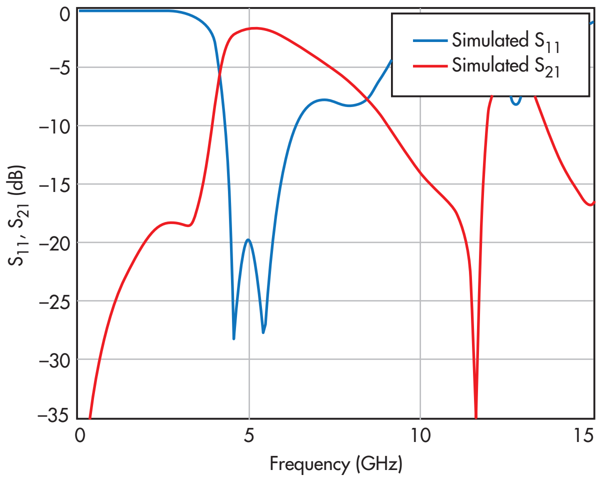

7. These traces show simulated S-parameters for the DGS BPF.

As *Fig. 7* shows, the results for the proposed bandpass filter were not very satisfactory. The passband loss is relatively high, while the absence of transmission zeros can be blamed for the lack of passband flatness and transition sharpness. To improve upon these shortcomings, a structure with a different topology was designed. An optimized structure was investigated by examining the impact of the external coupling between the feeds and the DGS resonators. This was done by shifting, step by step ,the microstrip feeds from the center of the structure to the edge of the structure, as shown in *Figs. 8 and 9*.

When the feed was moved from the center of the DGS to the edge, the filter characteristics were greatly improved *(Fig. 10)*. Optimum results were achieved when the feed positions were located on the edge of the DGS. By moving the feed positions to the edge of the DGS resonator and using a prober to control the distance, k_2, between the two feeds, a BPF with high selectivity can be produced *(Fig. 11)*.

The simulations of this modified filter reveal a center frequency, f_0, of 4.9 GHz, with a 3-dB bandwidth of approximately 280 MHz from 4.70 to 5.01 GHz. This filter design also shows low passband insertion loss of around 0.1 dB and excellent response symmetry. The filter design has two transmission zeros at 4 and 6 GHz, located close to the edges of the passband. This provides good selectivity and high stopband rejection for the BPF.

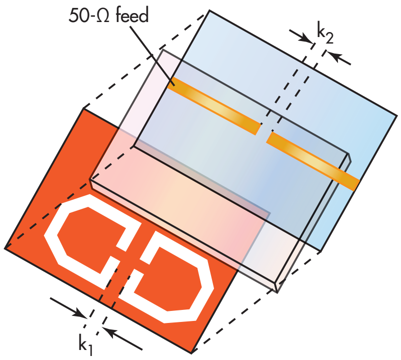

8. This is a 3D view of the DGS BF (with the feeds at the center).

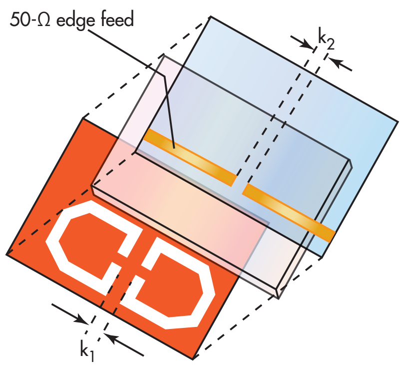

9. This is a 3D view of the DGS BF (with the feeds on the edges).

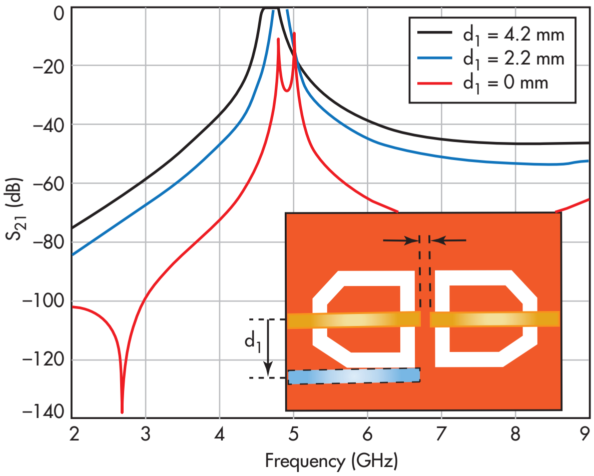

10. The S_{21} values are plotted for different values (in mm) of d_1.

To learn how to adjust the transmission zeros created in the lower and upper stopbands, and thus realize a desired passband bandwidth, as well as control sharp rejection characteristics, the effects of varying the width of gap k_2 on the transmission zeros were studied. *Figure 12* shows the dependence of J-inverter width k_2 on the positions of the transmission zeros. If all other parameters are kept constant and only k_2 is varied, it is relatively easy to control the position of the transmission zeros and the bandwidth and transition sharpness between passband and stopbands.

If k_2 increases, the positions of the upper and lower transmission zeros are shifted to higher and lower frequencies, respectively. Similarly, if k_2 decreases, the positions of the upper and lower transmission zeros are shifted to lower and higher frequencies, respectively.

To gain even greater insight into the filter design approach when using DGS resonators, a near-field distribution of the bandpass filter was computed *(Fig. 13)*. The filter's electric

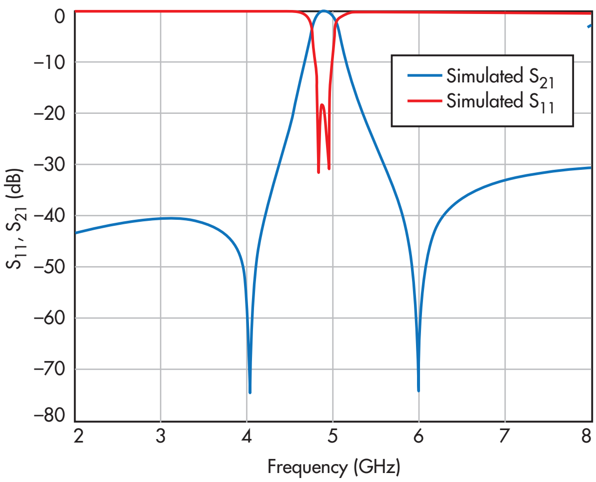

11. The traces show simulated S-parameters for the BPF.

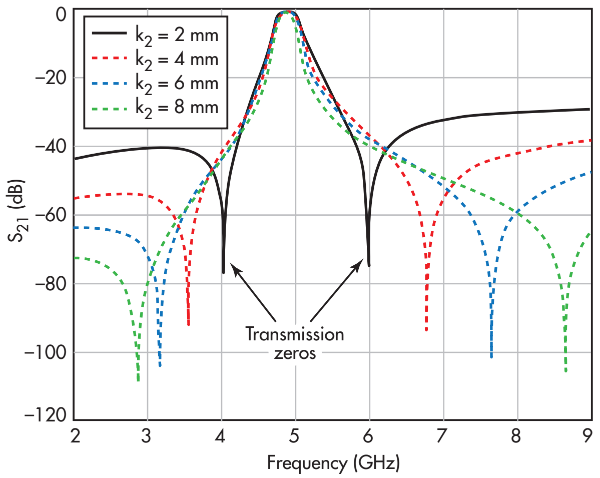

12. The plots show the S-parameters for different values of k_2 (in mm).

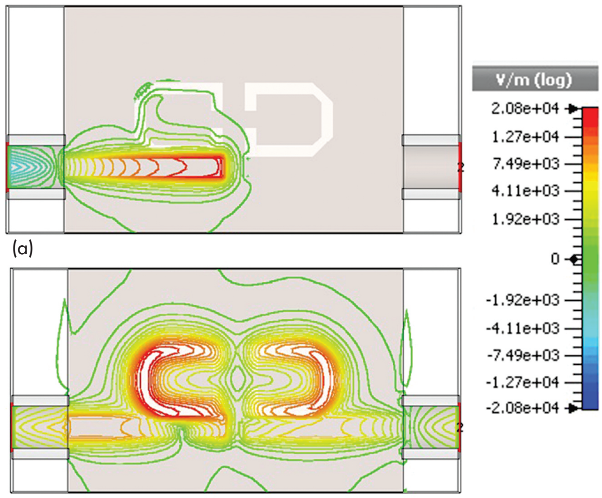

13. These are electric-field distribution results for the BPF: (a) in the stopband at 3.5 GHz and (b) in the passband at 4.8 GHz.

field was computed for two frequencies, in the passband and stopband regions. When at 3.5 GHz, the electric field exhibits high density around port 1 (the input feed port) with no energy flow around port 2, thus displaying strong stopband behavior *[Fig. 13(a)]*.

On the other hand, the electric field has high density at 4.8 GHz along the filter structure from ports 1 to 2 (across the DGS resonators) for good passband behavior *[Fig. 13(b)]*. The electric-field patterns indicate good coupling between the feeds and the DGS resonators.

In summary, the use of DGS resonators made it possible to design and fabricate compact filters in a microstrip. A simple transformation from a BSF to a BPF was achieved with the help of a J-inverter and some external coupling methods applied to the resonators.

FILTERING THROUGH FUNDAMENTAL SPECS

FILTERS HAVE LONG been a part of RF/microwave systems, as a means to isolate and separate signals in communications networks, radars, and other applications. Circuits such as bandpass filters (BPFs) and bandstop filters (BSFs) must often be specified for different applications, and selecting a "good fit" for a particular purpose is often more than simply searching for the smallest design possible. While the use of defected ground structures (DGSs) is one way to effectively shrink the size of a high-frequency BPF or BSF, a number of other specifications must be considered when sorting through RF/microwave filters from different suppliers.

BPFs and BSFs have considerably different functions; it therefore follows that their specifications will also be different. A BPF is typically judged by its passband characteristics, including passband insertion loss. Ideally, the passband insertion loss should be as low as possible and consistently low as possible across the full passband with no glitches. The BPF should provide as much rejection of unwanted signals as possible, both in its lower stopband and upper stopband outside of the low-loss passband. A BPF's passband insertion loss is also typically judged across an operating temperature range, and should remain as low as possible even when working at the highest temperatures within that range.

In contrast, an RF/microwave BSF is designed to remove signals from a certain band of frequencies within a system, while leaving signals outside of that stopband with little or no loss. Of course, every filter has limits on its total bandwidth, so this type of filter will be specified by the frequency range of its stopband as well as the frequency ranges of its upper and lower passbands. A BSF should provide a minimum amount of signal rejection in its stopband and minimal insertion loss in its passbands.

When attempting to shrink both types of filters, some laws of physics must still be obeyed, including the fact that handling power is generally a function of filter size and amount of loss. For example, a BPF that is designed for surface-mount packaging might simply be too small to handle continuous-wave (CW) power levels in excess of 50 W or more. If it suffers high insertion loss in its passband, the amount of power that it will handle will decrease as the amount of loss increases. Similarly, a bandstop filter will handle a certain amount of power based on its physical size, with smaller designs simply limited by the amount of heat they can dissipate.

The computer simulations performed on the filter circuits agree fairly well with measured results. They show that the use of DGS resonators offers great promise for the design of at least two types of compact microstrip filters. mw

REFERENCES

1. A. Boutejdar, A. Omar, and E. Burte, "LPF Builds On Quasi-Yagi DGS," Microwaves & RF, Vol. 52, No. 9, 2013.
2. Lung-Hwa Hsieh, "Tunable microstrip bandpass filters with two transmission zeros," IEEE Transactions on Microwave Theory & Techniques, Vol. 51 , No. 2, 2003, pp. 520-525.
3. A.A. Elrahman, A.Z. Eldein, A.A. Elmonem, and H. Fathi, "Small size defected ground structure (DGS) coupled resonator band pass filters with capacitor loaded slot using FDTD method," WSEAS Transactions on Communications, Vol. 10, No. 3, 2011, pp. 88-99.
4. A. Boutejdar, A. Omar, E.P. Burte, R. Mikuta, and A. Batmanov, "DGS and Multilayer Methods Make LPF," Microwaves & RF, Vol. 50, No. 3, 2011, pp. 61-72.
5. J.-S. Lim, Ch.-S. Kim, Y.-T. Lee, et al. "A new type of low pass filter with defected ground structure," Technical Program, European Microwave Week, Milan, Italy, September 24-26, 2002.
6. Adel B. Abdel-Rahman, Adel Z. El Dein, Hesham F.A. Hamed, and Ahmed A. Ibrahim, "Small Size Third order coupled resonator band-pass filter using capacitor loaded slots," IEEE Middle East Conference on Antennas and Propagation (MECAP), Cairo, Egypt, 2010.
7. A. Boutejdar, S. Amari, and A. Omar, "A novel compact J-Admittance inverter coupled microstrip bandpass filter using arrowhead shape as defected ground structure (DGS)," Microwave and Optical Technology Letters, Vol. 52, No. 1, January 2010, pp. 34-38.
8. Ahmed Boutejdar, "New Method to Transform Band-Pass to Low-Pass Filter Using Multilayer- and U-Slotted Ground Structure (SGS)-Technique," Microwave and Optical Technology Letters, Vol. 53, No. 10, October 2011, pp. 2427-2433.
9. A.K. Verma and A. Kumar, "Design of low-pass filters using some defected ground structures," AEU-International Journal of Electronics and Communications, Vol. 65, No. 10, 2011, pp. 864-872.
10. Mouloud Challal, A. Boutejdar, A. Azrar, and Danielle Vanhoenacker-Janvier, "Design of compact low-pass filter with large reject band using open circuit stubs and two-cascaded DGS quasi triangular resonators," Microwave and Optical Technology Letters, Vol. 55, 2013, pp. 122-127.
11. Dibakar Yadav, Tamasi Moyra, and Kaushik Debbarma, "Microstrip Hairpin Bandpass Filter with Improved Out of Band Performance", Emerging Trends in Computing and Communication Lecture Notes in Electrical Engineering, Vol. 298, 2014, pp. 27-32.
12. A. Abdel-Rahman, A. K. Verma, A. Boutejdar, and A.S. Omar, "Control of band-stop response of Hi-Lo microstrip low-pass filter using slot in ground plane," IEEE Transactions on Microwave Theory & Techniques, Vol. 52, March 2004, pp. 1008-1013.
13. A Boutejdar, "Design of broadstop band low pass filter using a novel quasi-Yagi-DGS-resonators and metal box-technique," Microwave and Optical Technology Letters, Vol. 56, No. 3, 2014, pp. 523-528.
14. A. Boutejdar and A. Omar, "Compensating For DGS Filter Loss," Microwaves & RF, Vol. 51, No. 2, 2012, pp. 68-76.
15. W.Q. Che, W.J. Feng, and K. Deng, "Microstrip dual-band bandstop filter of defected ground structure and stepped impedance resonators," International Journal of Electronics, Vol. 97, No. 11, 2010, pp. 1351-1359.
16. Jian-Kang Xiaoa and Yu-Feng Zhub, "Multiband bandstop filter using inner T-shaped defected microstrSip structure (DMS)," AEU International Journal of Electronics and Communications," Vol. 68, No. 2, February 2014, pp. 90-96.
17. Jia Shen, G. Hong, and M.J. Lancaster, Microstrip Filters for RF/Microwave Applications, second edition, (Wiley, New York, 2004).
18. A. Boutejdar, "New method to transform band-pass to lowpass filter using multilayer-and U-slotted ground structure-technique," Microwave and Optical Technology Letters, Vol. 53, No. 10, 2011, pp.